The Role of Intermittency in Internal-Wave Shear Dispersion

ERIC KUNZE

NorthWest Research Associates, Redmond, Washington

MILES A. SUNDERMEYER

School for Marine Science and Technology, University of Massachusetts Dartmouth, New Bedford, Massachusetts

(Manuscript received 11 July 2014, in final form 18 September 2015)

ABSTRACT

This paper revisits a long-standing discrepancy between (i) 1–5-km isopycnal diffusivities of $O(1)\,\mathrm{m^2\,s^{-1}}$ based on dye spreading and (ii) inferences of $O(0.1)\,\mathrm{m^2\,s^{-1}}$ from internal-wave shear dispersion $K_h \sim \langle K_z\rangle\langle V_z^2\rangle/f^2$ in several studies in the stratified ocean interior, where $\langle K_z\rangle$ is the bulk average diapycnal diffusivity, $\langle V_z^2\rangle$ the finescale shear variance, and f the Coriolis frequency. It is shown that, taking into account (i) the intermittency of shear-driven turbulence, (ii) its lognormality, and (iii) its correlation with unstable finescale near-inertial shear, internal-wave shear dispersion cannot necessarily be discounted based on available information. This result depends on an infrequent occurrence of turbulence bursts, as is observed, and a correlation between diapycnal diffusivity K_z and the off-diagonal vertical strain, or the vertical gradient of horizontal displacement, $|\boldsymbol{\chi}_z| = |\int \mathbf{V}_z\,dt|$, which is not well known and may vary from region to region. Taking these factors into account, there may be no need to invoke additional submesoscale mixing mechanisms such as vortical-mode stirring or internal-wave Stokes drift to explain the previously reported discrepancies.

1. Introduction

A number of tracer-release experiments in the ocean's stratified interior have reported 1–5-km horizontal diffusivities $K_h \sim O(1)\,\mathrm{m^2\,s^{-1}}$ (e.g., Ledwell et al. 1998; Sundermeyer and Ledwell 2001; D. A. Birch et al. 2015, unpublished manuscript). This is an order of magnitude larger than predictions for internal-wave shear dispersion $K_h \sim K_z|\boldsymbol{\chi}_z|^2$ based on Young et al. (1982), where $|\boldsymbol{\chi}_z| = |\int \mathbf{V}_z\,dt|$ and the vertical shear $\mathbf{V}_z = (u_z, v_z) = (\partial u/\partial z, \partial v/\partial z)$. These shear-dispersion predictions have been based on average diapycnal diffusivities $\langle K_z\rangle$, average near-inertial shear variances $\langle V_z^2\rangle$, or both—that is, $K_h \sim \langle\langle K_z\rangle V_z^2\rangle/f^2 = \langle K_z\langle V_z^2\rangle\rangle/f^2 = \langle K_z\rangle\langle V_z^2\rangle \le \langle K_z\rangle 4N^2/(2f^2) \sim O(0.1)\,\mathrm{m^2\,s^{-1}}$ for a canonical open-ocean internal-wave field.

To explore a possible reason for this order-of-magnitude discrepancy, this paper examines the consequences of recognizing that $\langle K_z|\boldsymbol{\chi}_z|^2\rangle = \langle K_z\rangle\langle|\boldsymbol{\chi}_z|^2\rangle + \langle K_z'|\boldsymbol{\chi}_z|^{2\prime}\rangle$ will exceed $\langle K_z\rangle\langle|\boldsymbol{\chi}_z|^2\rangle$ if K_z and $|\boldsymbol{\chi}_z|^2$, both of which are positive definite, are intermittent and positively correlated. This may be the case in the ocean where finescale near-inertial waves provide background variances $\langle V_z^2\rangle \sim O(N^2)$ and $\langle|\boldsymbol{\chi}_z|^2\rangle \sim O(N^2/f^2)$ but sporadically become unstable ($V_z^2 > 4N^2$) to produce nonzero turbulent diapycnal diffusivities K_z.

Section 2 provides background on internal-wave shear dispersion; section 3 discusses modifications arising from intermittency, lognormality, and correlation between turbulence and unstable shear; and section 4 summarizes the results.

2. Background

Shear dispersion in the ocean results from coupling between (i) vertically differential horizontal displacements (off-diagonal vertical strain) $|\boldsymbol{\chi}_z| = |\int \mathbf{V}_z\,dt|$ arising from vertical shear $\mathbf{V}_z = (u_z, v_z)$, and (ii) diapycnal turbulent mixing K_z (Young et al. 1982) As illustrated in Fig. 1, horizontal mixing is most effectively accomplished when diapycnal mixing coincides with maximal $|\boldsymbol{\chi}_z|$. This can be understood from the geometrical derivation in section 2c of Young et al. (1982). Diapycnal

Corresponding author address: Eric Kunze, NorthWest Research Associates, 4126 148th Ave. NE, Redmond, WA 98052.
E-mail: kunze@nwra.com

DOI: 10.1175/JPO-D-14-0134.1

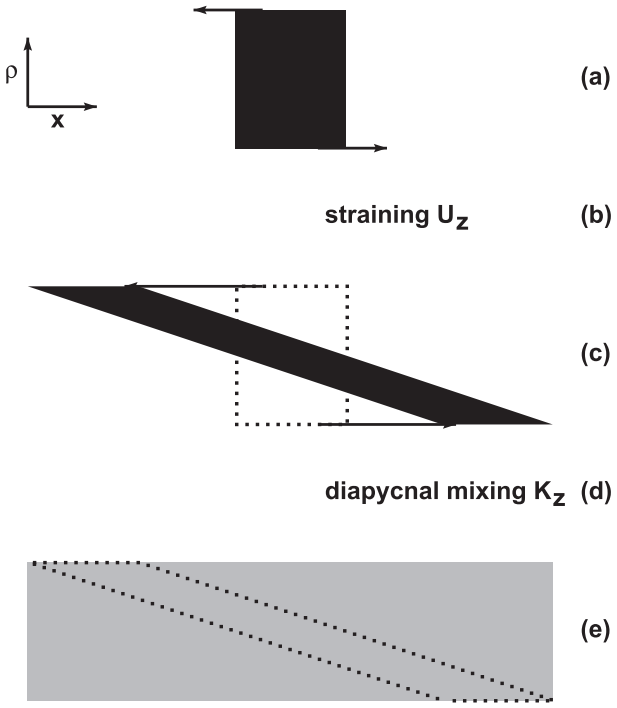

FIG. 1. Sequence illustrating the steps involved in internal-wave shear dispersion in a 2D vertical plane. When (a) a horizontal property gradient experiences (b) oscillating vertical shear U_z, it is (c) strained to produce vertical gradients. If (d) diapycnal mixing K_z then occurs when the off-diagonal vertical strain $X_z = \int U_z\,dt$ is maximal (c), then (e) horizontal mixing is maximized by the diapycnal dilution. At each step, the state in the preceding step is shown as dotted.

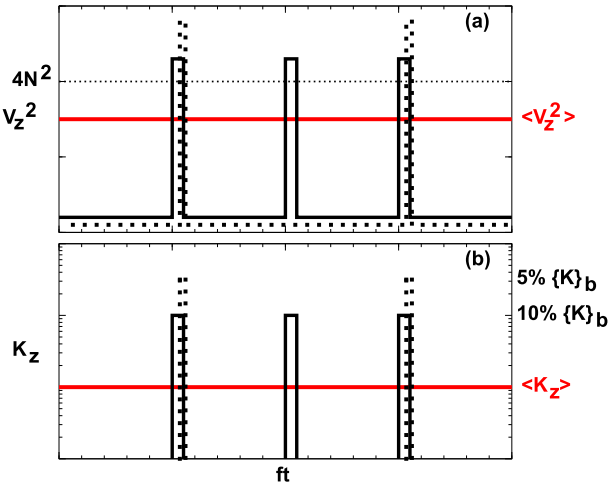

FIG. 2. Schematic time series of (a) shear variance V_z^2 and (b) diapycnal diffusivity K_z assuming the usual application of internal-wave shear dispersion based on constant $\langle V_z^2 \rangle$ and $\langle K_z \rangle$ as in (4) (red), and displaying the actual intermittency of turbulence K_z and its correlation with unstable instantaneous finescale shear variance V_z^2 as in (11) (black). Solid and dotted curves in black correspond to 10% and 5%, respectively, intermittency of turbulent events with burst average $\{K_z\}_b$ levels labeled on the right axis. The horizontal time axis has been normalized with the Coriolis frequency f and is deliberately not quantified for lack of observational information.

diffusivity K_z will not act on vertically aligned isolines—that is, $\theta_x = \partial\theta/\partial x$ (Fig. 1a)—but will act when these isolines are tilted by vertical shear U_z (Fig. 1b) to form vertical gradients—for example, $\theta_z = \int \theta_{zt}\,dt = -\int u_z \theta_x\,dt = -X_z\theta_x$ (Fig. 1c), where X_z is the x component of the off-diagonal vertical strain. Since internal-wave off-diagonal vertical strain is dominated by finescale near-inertial waves, it is rotary with $X_z = \int u_z\,dt$ and $Y_z = \int v_z\,dt$ out of phase by 90°. As further explained by Young et al., the vertical shear also elongates isolines (Fig. 1) so that the projection of this elongation in the vertical likewise goes as X_z. Thus, the diffusive flux due to vertical diffusion can instantaneously be expressed as $K_z X_z^2 \theta_x$, where $K_z X_z^2$ plays the role of a horizontal diffusivity, implying an average horizontal diffusivity of the form $\langle K_z X_z^2 \rangle$ as described in section 3a. In the Young et al. case of constant vertical diffusivity $\langle K_z \rangle$, the resulting average horizontal diffusivity is $\langle K_z \rangle \langle X_z^2 \rangle$ in the oceanic limit of $K_z m^2 \ll f$ (see below). Internal-wave shear dispersion based on *average* diapycnal diffusivities $\langle K_z \rangle$ and *average* shear variances $\langle V_z^2 \rangle = \langle u_z^2 \rangle + \langle v_z^2 \rangle$ (red lines in Fig. 2) is more completely expressed as

$$K_h = \frac{\langle K_z \rangle \langle V_z^2 \rangle}{\omega^2} \left(\frac{1}{1 + \dfrac{\langle K_z \rangle^2 m^4}{\omega^2}} \right), \tag{1}$$

where ω is the wave frequency and m is the vertical wavenumber. Derivation of (1) can be found in Young et al. (1982) under various conditions for constant $\langle K_z \rangle$. The constraint of constant diapycnal diffusivity and shear variance will be relaxed here in section 3a.

For internal waves, the largest contributions to (1) are from finescale near-inertial waves, which have minimum frequency $\omega = f$ and contain the bulk of the shear variance $\langle V_z^2 \rangle$ near rolloff vertical wavenumber $m = m_c = 0.2\pi\,\mathrm{rad\,m^{-1}}$ [corresponding to a vertical wavelength $\lambda_c = 2\pi/m_c = 10\,\mathrm{m}$ and a length scale $L_c = 1/m_c = \lambda_c/(2\pi) = 1.6\,\mathrm{m}$ for typical ocean conditions]. Thus, finescale near-inertial waves have the maximal internal-wave off-diagonal vertical strain variance $\langle |\boldsymbol{\chi}_z|^2 \rangle = \langle |\mathbf{V}_z|^2 \rangle / f^2$. In (1), the second term in the denominator of the ratio in parentheses—that is $\langle K_z^2 \rangle m^4 / f^2$—represents diffusive smoothing of small-scale vertical structure that acts to short-circuit lateral dispersion if vertical diffusion is large. For a canonical midlatitude deep-ocean internal-wave field with $\langle K_z \rangle \sim 0.05 \times 10^{-4}\,\mathrm{m^2\,s^{-1}}$ (Gregg 1989) and $m_c \sim 0.2\pi$ (Gargett et al. 1981), poleward of 0.5° latitude the second term in the denominator is three

orders of magnitude smaller than the first so it can be neglected for all practical purposes.[1]

Moreover, since $m_c \sim E^{-1}$ (Gargett et al. 1981; Gargett 1990; Polzin et al. 1995) and $\langle K_z \rangle \sim E^2$ (Henyey et al. 1986; D'Asaro and Lien 2000), where E is the nondimensional spectral energy level of the internal-wave field, $\langle K_z \rangle m^2$ is invariant so that the second term remains small compared to the first for *all* internal-wave-driven mixing. Finally, if $\langle K_z \rangle m^2$ should become comparable or greater than f, then the shear in wavenumber m would be smoothed away in less than an inertial period to restore the $\langle K_z \rangle m^2 \ll f$ state because the shear-containing m has been reduced. We conclude that the ocean is in the weak-mixing limit corresponding to (37a) in Young et al. (1982). Since the $O(10^{-3})$ correction associated with the parenthetic term in (1) is not significant, (1) can be approximated to within a few percent as

$$K_h = \frac{\langle K_z \rangle \langle |\mathbf{V}_z|^2 \rangle}{f^2} = \frac{\langle K_z \rangle \langle V_z^2 \rangle}{f^2} \tag{2}$$

or more physically as

$$K_h = \langle K_z \rangle \langle |\boldsymbol{\chi}_z|^2 \rangle, \tag{3}$$

where $\langle |\boldsymbol{\chi}_z|^2 \rangle = \langle X_z^2 + Y_z^2 \rangle = \langle u_z^2 + v_z^2 \rangle / f^2$ is the variance of the vertical gradient of horizontal displacement $\boldsymbol{\chi} = (X, Y)$—that is, the two off-diagonal components of the vertical strain, or deformation, tensor $\nabla \boldsymbol{\chi} = \int (\nabla \mathbf{V})\, dt$ (Kundu and Cohen 2004). Equation (3) and Fig. 1 illustrate that, physically, dispersion is better described as coupling of diapycnal diffusion K_z and off-diagonal vertical strain $|\boldsymbol{\chi}_z| = |\int \mathbf{V}_z\, dt|$, rather than vertical shear $V_z = |\mathbf{V}_z|$. Thus, it might more aptly be referred to as "strain dispersion," but we will use the term "shear dispersion" for consistency with the literature.

Estimates of internal-wave-driven horizontal diffusivity K_h based on (2) in the literature use either $\langle K_z \rangle$, $\langle V_z^2 \rangle$, or both (red lines in Fig. 2) following Young et al. (1982). This amounts to assuming that fluctuations in the turbulent diapycnal diffusivity and shear variance are uncorrelated, that is, $\langle K_z' V_z^{2\prime} \rangle = 0$. Thus, for an internal-wave field that is stable on average with $\langle V_z^2 \rangle \le \delta_c^2 N^2/2$,

$$K_h = \frac{\langle K_z \rangle \langle V_z^2 \rangle}{f^2} \le \frac{\langle K_z \rangle N^2}{2 f^2} \delta_c^2, \tag{4}$$

where δ_c is the critical gradient Froude number. For canonical midlatitude upper pycnocline values of $\langle K_z \rangle = 0.05 \times 10^{-4}\,\mathrm{m^2\,s^{-1}}$, $N = 10^{-2}\,\mathrm{rad\,s^{-1}}$, $f = 10^{-4}\,\mathrm{rad\,s^{-1}}$, and $\delta_c = 2$, K_h based on (4) can be no more than $\sim 0.1\,\mathrm{m^2\,s^{-1}}$.

Several field studies have compared internal-wave shear dispersion [(4)] with submesoscale dye dispersion. Tracer studies in the North Atlantic subtropical gyre (Ledwell et al. 1998) used upper-bound $\langle K_z \rangle$ inferred from tracer and a shear spectrum based on moored current-meter measurements to infer internal-wave shear dispersion from (2) of $K_h < 0.024\,\mathrm{m^2\,s^{-1}}$, more than a factor of 2 smaller than the 1–10-km dye lateral diffusivity of $0.07 \pm 0.04\,\mathrm{m^2\,s^{-1}}$ 14 days after release, and nearly two orders of magnitude smaller than the dye lateral diffusivity of $0.6–6\,\mathrm{m^2\,s^{-1}}$ estimated 5–6 months after release. Similar discrepancies were reported in 5–10-km tracer patches sampled over 3–5 days on the New England continental shelf (Sundermeyer and Ledwell 2001). Using dye-based $\langle K_z \rangle$ and relative lateral displacements with depth $|\boldsymbol{\chi}_z|$ inferred from shipboard ADCP time series, shear dispersion [(2)] in two of four tracer releases was nearly an order-of-magnitude smaller than dye-based lateral diffusivities, which ranged from 0.1–0.6 to $3–7\,\mathrm{m^2\,s^{-1}}$, with the other two releases showing closer agreement between dye and shear dispersion. Finally, shear dispersion using $\langle K_z \rangle$ was again an order-of-magnitude smaller than the 1–10-km lateral dye diffusivities over 6 days of $0.5–4\,\mathrm{m^2\,s^{-1}}$ in the summer pycnocline of the Sargasso Sea (Shcherbina et al. 2015; D. A. Birch et al. 2015, unpublished manuscript). The discrepancy between dye and shear-dispersion estimates is by no means universal as other studies ranging in duration from a few hours to 1–2 days have found closer agreement (e.g., Inall et al. 2013; Moniz et al. 2014). Common to all the aforementioned studies is that they did not account for the intermittency of diapycnal turbulent mixing events and their possible correlation with the off-diagonal vertical strain $|\boldsymbol{\chi}_z| = |\int \mathbf{V}_z\, dt|$.

The apparent failure of internal-wave shear dispersion to explain observed isopycnal mixing in some studies has fostered a number of alternative hypotheses. Smith and Ferrari (2009) examined eddy shear dispersion in a quasigeostrophic (QG) numerical simulation in a baroclinically unstable QG model that reproduced filaments of similar $O(1)$-km horizontal scale to those observed in the ocean (Ledwell et al. 1998). Their lateral diffusivity scaled as $K_h \sim K_z N^2/f^2$ like (4), so it still falls short of observed dye diffusivities by more than an order of magnitude, though they noted considerable scatter in the aspect ratio of filaments about N/f. The Smith and Ferrari model did not include internal waves or unbalanced subinertial flows as might arise in a primitive equation model (e.g., Molemaker et al. 2010). These non-QG flows must be present on the submesoscale based on surface drifter-pair

[1] This term plays a role in limiting horizontal mixing for subinertial ($\omega \ll f$, e.g., vortical mode) shears to $\langle V_z^2 \rangle / (K_z m^4) \sim N^2 \delta_g^2 / (K_z m^4)$, where δ_g is the geostrophic gradient Froude number. For the abovementioned values of K_z and m, and vortical-mode gradient Froude number $\delta_g \ll 1$ as reported by Pinkel (2014), subinertial shear dispersion is much less than $1\,\mathrm{m^2\,s^{-1}}$.

spreading (Lumpkin and Elipot 2010; Poje et al. 2014) and horizontal wavenumber spectra of submesoscale water-mass anomalies on isopycnals (Rudnick and Ferrari 1999; Cole and Rudnick 2012; Kunze et al. 2015).

It has also been proposed that horizontal dispersion might arise from Stokes drift in a dissipative weakly nonlinear internal-wave field (Bühler et al. 2013) or from stirring by finescale potential vorticity anomalies (Lelong et al. 2002; Sundermeyer et al. 2005; Lelong and Sundermeyer 2005; Sundermeyer and Lelong 2005) termed the vortical mode (Müller 1984). Kinematic arguments and numerical simulations indicate that vortical-mode stirring should be more effective than vortical-mode shear dispersion, and that this stirring may be enhanced by upscale energy transfer of vortical-mode (PV) variance (Sundermeyer et al. 2005; Brunner-Suzuki et al. 2014). Direct measurement of finescale vortical mode in the ocean has proven challenging and inconclusive (Müller et al. 1988; Kunze et al. 1990a; Kunze and Sanford 1993; Kunze 1993; Polzin et al. 2003) because of the dominance of internal waves in dynamic (horizontal kinetic and available potential energy) signals on these scales and the resulting demands on sampling to avoid space–time aliasing. However, recently, Pinkel (2014) reported that subinertial finescale potential vorticity is dominated by finescale fluctuations in stratification N^2 and that subinertial vertical shear is many orders of magnitude below near-inertial shear so unlikely to contribute significantly to shear dispersion.

3. Intermittency

Here, we revisit internal-wave shear dispersion, taking into account the observed intermittency of K_z, including its lognormal distribution, and its possible correlation with finescale off-diagonal components of vertical strain $\boldsymbol{\chi}_z = \int \mathbf{V}_z\, dt$. Ocean turbulence is sporadic (black curves in Fig. 2), typically only occupying 5%–10% of space–time in the pycnocline (Gregg and Sanford 1988). Nonzero turbulent dissipation rates are also approximately lognormally distributed (Gregg et al. 1993; Davis 1996). In the stratified interior, turbulence is largely driven by finescale $O(1)$-m internal-wave shear (Eriksen 1978; Desaubies and Smith 1982; Polzin 1996), so unstable shears are also intermittent and present 5%–10% of the time (Kunze et al. 1990b). While shears are not correlated with turbulence when they are stable, or when unstable scales are not resolved (Gregg et al. 1986; Toole and Schmitt 1987), resolved unstable instantaneous finescale shears $V_z > 2N$ on $O(1)$ m scales exhibit strong correlation with turbulent dissipation rates ε as described in section 3c.

a. *Theoretical shear dispersion with intermittent shear-driven turbulent mixing*

Starting from the horizontal advection–diffusion equation for a conservative tracer θ,

$$\frac{D\theta}{Dt} = \theta_t + u\theta_x = K_z\theta_{zz} \tag{5}$$

with idealized initial condition $\theta(x, z, 0) = \cos(kx)$ from which more general realistic initial conditions can be constructed (Young et al. 1982), we model intermittent (r of the time) mixing K_z as

$$K_z = \frac{\langle K_z \rangle}{r}\Pi(t - t_n) \tag{6}$$

due to sporadically unstable near-inertial shear u, defined as

$$\begin{aligned} u &= u_z z\cos(ft) + u_z' z\cos(ft)\Pi(t - t_n) \\ &= N\delta_c z\cos(ft) + N(\delta_N - \delta_c)z\cos(ft)\Pi(t - t_n) \end{aligned} \tag{7}$$

as illustrated in Fig. 1, where the gradient Froude number $\delta_N = |\mathbf{V}_z|/N$ and δ_c is the critical threshold value. The u_z term represents the $O(N)$ background shear and the u_z' term represents excess shear-associated turbulent bursts. Shear-driven turbulent bursts are modeled with a boxcar function $\Pi(t - t_n)$ of average duration δt that is nonzero every $\Delta t = \delta t/r$ on average, that is, $t_n \sim n\Delta t$. The z dependence in (7) is valid in the weak-mixing limit of Young et al. (1982), which was argued in section 2 to be appropriate for midlatitude ocean internal waves, but this approximation will not hold on the equator or for finescale subinertial shears. Integrating (7), the horizontal displacement is

$$\begin{aligned} X = \int u\, dt &= \frac{N\delta_c z}{f}\sin(ft) \\ &+ \sum_n \frac{N(\delta_N - \delta_c)z}{f}\{\sin[f(t_n + \delta t)] - \sin(ft_n)\}, \end{aligned} \tag{8}$$

which, when substituted in as the advective coordinate x in the tracer initial condition, yields

$$\begin{aligned} \theta(x, z, t) = \Theta(t)\cos\Bigg\{k\Bigg[&\frac{N\delta_c z}{f}\sin(ft) \\ &+ \sum_n \frac{N(\delta_N - \delta_c)z}{f}\{\sin[f(t_n + \delta t)] - \sin(ft_n)\}\Bigg]\Bigg\}, \end{aligned} \tag{9}$$

so that the tracer evolution proceeds as

$$\frac{D\Theta}{Dt} = -\frac{\langle K_z\rangle \Pi(t-t_n)}{r}\left[\frac{N\delta_c}{f}\sin(ft) + \sum_n \frac{N(\delta_N-\delta_c)}{f}\{\sin[f(t_n+\delta t)]-\sin(ft_n)\}\right]^2 k^2\Theta(t). \tag{10}$$

This is in the form of a diffusion equation with average horizontal diffusivity K_h given by the average of the coefficient in front of $k^2\Theta$ on the right-hand side,

$$K_h = \langle K_z\rangle \frac{N^2}{2f^2}[\delta_c^2 + 4(\delta_N-\delta_c)^2 H(\delta_N-\delta_c)\sin^2(f\delta t)], \tag{11}$$

where $H(\cdot)$ is the Heaviside function. The first term in (11) corresponds to shear dispersion associated with $\langle K_z\rangle$ and background shear variance $u_z^2 = \langle V_z^2\rangle = N^2\delta_c^2/2$ found by Young et al. (1982). The second term arises from excess unstable shear $N^2\delta_N^2 > N^2\delta_c^2$ associated with turbulent bursts. The second term can be an order of magnitude larger than the first for $\delta_N \sim (2\text{–}3)\delta_c$, depending on the statistics of turbulence and the relationship between shear and turbulence as laid out in section 3d. Whether the second term dominates will depend on the duration δt of the unstable shear and mixing events since it takes $O(f^{-1})$ for elevated shear to express itself as elevated off-diagonal vertical strain $|\boldsymbol{\chi}_z| = |\int \mathbf{V}_z\, dt|$. Since $(X_z, Y_z) = \int (u_z, v_z)\, dt$, there is no guarantee that large strain $|\boldsymbol{\chi}_z|$ will coincide in time with large K_z. While there are no measured correlations between $|\boldsymbol{\chi}_z|^2$ and K_z, with some observationally based caveats noted below, it may be possible to use correlations between V_z^2 and K_z, that is, $K_h \sim \langle K_z V_z^2\rangle/f^2$ as described next. However, we emphasize that off-diagonal vertical strain $|\boldsymbol{\chi}_z|$ is the physically relevant variable.

b. *Properties of observed finescale shear*

Finescale shear layers have low aspect ratios and cross isopycnals with gentle slopes, consistent with near-inertial waves (Itsweire et al. 1989). This is mirrored in the aspect ratios of turbulent layers (Marmorino et al. 1986; Marmorino et al. 1987), which can persist for many inertial time scales f^{-1} (Gregg et al. 1986; Sundermeyer et al. 2005). Because group velocities are small at the 10-m vertical wavelengths that dominate internal-wave shear, these waves cannot propagate from the surface or bottom but likely arise in situ from wave–wave or wave–mean flow interactions that transfer wave variance from lower to higher vertical wavenumber m on time scales such as $m(kU_z)^{-1} \sim N(\omega^2 - f^2)^{-1/2}/N \sim (\omega^2 - f^2)^{-1/2}$ based on ray-tracing theory. The most relevant interactions for production of unstable shear can occur on time scales much shorter than f^{-1} (Sun and Kunze 1999) so that interpreting the resulting shears from linear internal-wave theory may be inappropriate. Whether unstable shear $|\mathbf{V}_z| > \delta_c N$ and mixing persist long enough to produce a correlation between large vertical gradients of horizontal displacement $|\boldsymbol{\chi}_z| = |\int \mathbf{V}_z\, dt|$ and K_z remains an open question that we discuss in the appendix and revisit in the summary.

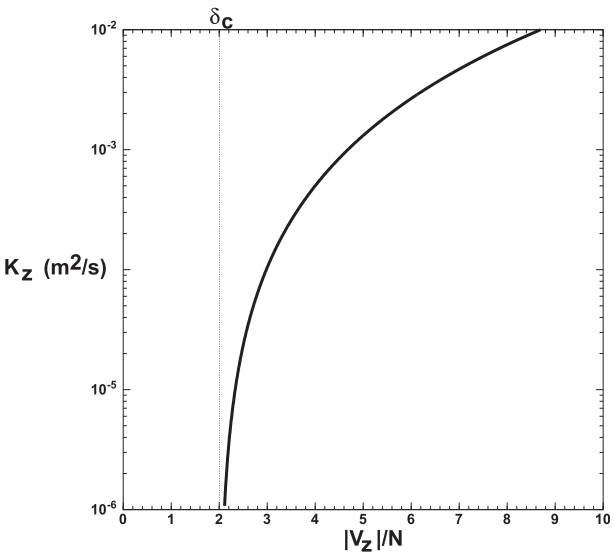

FIG. 3. Shear-driven inferred turbulent diapycnal diffusivity K_z from (12) as a function of gradient Froude number $\delta_N = |\mathbf{V}_z|/N$ assuming a critical gradient Froude number $\delta_c = 2$, $N = 10^{-2}$ rad s^{-1}, $\Delta z = 1$ m, and $\gamma = 0.2$.

c. *Relation between unstable shears and turbulence*

To evaluate (11), we relate instantaneous K_z to V_z^2 using the unstable shear parameterization proposed by Kunze et al. (1990b) and observationally supported by Peters et al. (1995), Polzin (1996), and Jurisa et al. (2015, manuscript submitted to *J. Phys. Oceanogr.*),

$$\varepsilon = \left(\frac{\Delta z^2}{96}\right)(V_z^2 - \delta_c^2 N^2)(|\mathbf{V}_z| - \delta_c N)H(|\mathbf{V}_z| - \delta_c N) = \left(\frac{N^3\Delta z^2}{96}\right)(\delta_N+\delta_c)(\delta_N-\delta_c)^2 H(\delta_N-\delta_c) \tag{12}$$

(Fig. 3), where Δz is the vertical scale used to estimate shear V_z and buoyancy frequency N estimates, and $H(\cdot)$ is the Heaviside function to account for the fact that turbulent dissipations only arise for supercritical shear. Parameterization (12) is made up of two components: (i) the available horizontal kinetic energy in the unstable shear $(V_z^2 - \delta_c^2 N^2)\Delta z^2/24$ and (ii) the Kelvin–Helmholtz

growth rate in the initial shear instability $(|\mathbf{V}_z| - \delta_c N)/4$ (Hazel 1972), which we equate to the rate at which unstable kinetic energy is lost to turbulence production. The exact model used is not critical provided the dissipation rate ε is an increasing function of V_z^2—for example, Mellor and Yamada (1982) could also be used. But finescale parameterizations like Gregg et al. (2003) or MacKinnon and Gregg (2003) are not suitable because they are based on average variances. The "instantaneous" vertical diffusivity $K_z = \gamma\varepsilon/\langle N^2\rangle$, where γ is the mixing efficiency (Osborn 1980), must be based on dissipation rates ε averaged over a turbulent growth and decay event on a time scale $O(N^{-1})$ to be meaningful, and this same averaging must be applied to the unstable or reduced shear $(|\mathbf{V}_z| - \delta_c N) > 0$. The vertical scale Δz must be small enough to resolve unstable shear but not so small to capture the outer scales of turbulence; scale separation of these (Kunze 2014) ensures this is possible provided that unstable $|\mathbf{V}_z|/N$ is not too large. Polzin (1996) argued that (12) was robust to changes in Δz provided that $\langle V_z^2\rangle/\langle N^2\rangle = \langle(\Delta V/\Delta z)^2\rangle/\langle N^2\rangle \sim O(1)$; an iterative procedure might be more effective for heterogeneous turbulence environments. A critical gradient Froude number $\delta_c = 2$ is consistent with laboratory (Thorpe 1971; Scotti and Corcos 1972; Rohr et al. 1988) and numerical (Itsweire et al. 1993) turbulence studies, but values of 1.7–2 give similar results (Polzin 1996).

Peters et al. (1995) reported that 2-m estimates of ε parameterized from (12)—that is, shear $|\mathbf{V}_z|$, or rather reduced shear $|\mathbf{V}_z| - \delta_c N$—both (i) reproduced average microstructure dissipation rate $\langle\varepsilon\rangle$ and (ii) were significantly correlated with instantaneous microstructure ε with $R \sim 0.6$, which is likely a lower bound given problems associated with instrument noise in the 2-m shear estimate. Polzin (1996) found that (12) was as good a predictor of average dissipation rate ε as a finescale parameterization based on internal wave–wave interaction theory (Henyey et al. 1986; Gregg 1989; Polzin et al. 1995). More importantly, (12) reproduced the behavior of ε as a function of N and V_z (Polzin 1996, his Figs. 2 and 3), again indicating a strong correlation between unstable shear and turbulent mixing. The observed consistency of (12) with microstructure measurements indicates that turbulence and unstable shear occupy the same 5%–10% of space/time.

While (12) suggests that unstable shear should be removed on a time scale $\delta t \sim 4/(|\mathbf{V}_z| - \delta_c N) \sim O(N^{-1}) \ll O(f^{-1})$, as also inferred from the ratio of turbulent energy variance to dissipation rates (Dillon 1982; Moum 1996), this is too rapid to allow large vertical gradients of horizontal displacement $|\boldsymbol{\chi}_z| = |\int \mathbf{V}_z\, dt|$ to develop. On the other hand, microstructure time series measurements often find that more persistent turbulent patches associated with near-inertial shear dominate mixing (Gregg et al. 1986; Sundermeyer et al. 2005). This is only possible if unstable shears $|V_z| > \delta_c N$ are being continuously replenished by nonlinear wave–wave interactions or wave–mean flow interactions to create a succession of $O(N^{-1})$ turbulent bursts over longer durations δt; that is,

$$\frac{\partial(V_z^2)}{\partial t} = \alpha V_z^2 - \sigma V_z^2 \ll N V_z^2, \tag{13}$$

where α is the replenishment rate by nonlinear interactions (refer to the appendix) and $\sigma = (|\mathbf{V}_z| - \delta_c N)/4$ is the rate of loss to turbulence. Maintenance of unstable shears for durations of $O(f^{-1})$ or longer would allow time for production of large $|\boldsymbol{\chi}_z| = |\int \mathbf{V}_z\, dt|$, while diapycnal turbulent mixing K_z remains elevated [(11)].

d. *Statistical prediction of shear dispersion with intermittency*

To account for turbulence intermittency $r \in [0, 1]$, instantaneous K_z is assumed to be zero for $1 - r$ of the time [assuming molecular diffusivity κ to be negligible compared to $\langle K_z\rangle$ (Fig. 2)] and to have burst averages $\{K_z\}_b = \langle K_z\rangle/r$ for the r of the time it is nonzero; that is, $\{\cdot\}_b$ represents the average during the turbulent bursts and K_z is composed of two populations, one is uniformly zero for $1 - r$ fraction of the time and the other has a lognormal distribution and mean $\{K_z\}_b = \langle K_z\rangle/r$ for r of the time (Fig. 2b). Bursts are not necessarily limited to be of $O(N^{-1})$ duration but may persist for many inertial time scales (Gregg et al. 1986; Sundermeyer et al. 2005). For the r of the time K_z is nonzero, K_z is taken to have a lognormal probability density function as is observed to be approximately true (e.g., Gregg et al. 1993)

$$\mathrm{PDF}(K_z) = \frac{1}{\sqrt{2\pi}\sigma_{\ln K} K_z} \exp\left\{\frac{-[\ln(K_z) - \{\ln(K_z)\}_b]^2}{2\sigma_{\ln K}^2}\right\} \tag{14}$$

with two parameters: (i) the physically meaningful $\ln(\{K_z\}_b) = \{\ln(K_z)\}_b + \sigma_{\ln K}^2/2$, where $\{K_z\}_b = \langle K_z\rangle/r$; and (ii) the standard deviation of $\ln(K_z)$, $\sigma_{\ln K}$, where $\sigma_{\ln K}^2 = \ln(1 + \{K_z^2\}_b/\{K_z\}_b^2)$. Shear dispersion (11) can then be reexpressed as

$$K_h = \frac{\langle K_z\rangle\langle V_z^2\rangle}{f^2} + \mathrm{corr}\,\frac{2r}{f^2}\int K_z[V_z^2(K_z) - \langle V_z^2\rangle]\mathrm{PDF}(K_z)\, dK_z, \tag{15}$$

taking advantage of $\langle xy'\rangle = \langle(\langle x\rangle + x')y'\rangle = \langle\langle x\rangle y'\rangle + \langle x'y'\rangle = \langle x'y'\rangle$ in the second rhs term and letting corr

represent $\langle \sin^2(f\delta t)\rangle$ as well as ocean K_z and V_z/N not lying on the curve shown in Fig. 3 from (12). It is possible that corr is a function of V_z/N so it should be inside the integral, but there is insufficient observational information to assess this at this time. As before, the first rhs term in (15) represents horizontal mixing associated with the background ubiquitous shear variance $\langle V_z^2\rangle \sim O(\delta_c^2 N^2/2)$ (Young et al. 1982), while the second is due to the turbulent bursts that are present r of the time and which we are assuming to have correlation corr with unstable shears (Fig. 2a). For the second term, shear variance V_z^2 (K_z) is obtained numerically from (12) and the PDF from (14). Choosing a standard deviation $\sigma_{\ln K}$ is more challenging as this is rarely reported. Theoretically, it should have an upper bound of 2.57 for random internal-wave breaking (Gregg et al. 1993). But ocean turbulence is neither stationary nor homogeneous. After correcting for instrument noise, Gregg et al. (1993) found $\sigma_{\ln K} = 1.2$ in a dataset with a canonical [Garrett–Munk (GM)] level internal-wave field and 1.5 in a dataset 4 times more energetic. Baker and Gibson (1987) reported $\sigma_{\ln\varepsilon}$ or $\sigma_{\ln\chi}$ ranging from 1.30 to 2.53 in seven off-equatorial microstructure measurement datasets. We caution that ocean turbulence is unlikely to be perfectly lognormal because of the nonstationarity of the background environment and forcing, both failing to satisfy underlying homogeneity assumptions in statistical theories of turbulence (Davis 1996); however, insufficient information is available to determine a robust observationally based PDF. Since (15) is sensitive to the high-K_z tail, which is not well characterized observationally, it might easily over- or underestimate K_h. Thus, the results reported below are highly speculative and require observational testing.

The principal variables affecting (16) are (i) the intermittency r, (ii) assumed lognormality PDF(K_z), and (iii) correlation corr, as explored in Fig. 4 and Table 1, which show K_h depending roughly as $r^{-1/2}$ on intermittency r. For perfect shear-turbulence correlation (corr = 1; thick solid curves, Fig. 4) in the continuous turbulence limit ($r = 1$), the horizontal diffusivity $K_h \sim 0.2\,\mathrm{m^2\,s^{-1}}$ for $\sigma_{\ln K} = 1.2$ and $K_h \sim 0.52\,\mathrm{m^2\,s^{-1}}$ for $\sigma_{\ln K} = 2.1$, boosted by lognormality alone from $\langle K_z\rangle\langle V_z^2\rangle/(2f^2) = 0.18\,\mathrm{m^2\,s^{-1}}$ corresponding to no intermittency and no lognormality (thin solid line at $r = 1$). As $r \to 0$, the inferred horizontal diffusivity K_h increases sharply. For typical low ocean intermittencies, $r = 0.05$–0.1, $\sigma_{\ln K} = 1.2$, and corr = 1 (Fig. 4); isopycnal diffusivity $K_h \sim 0.4$–$0.6\,\mathrm{m^2\,s^{-1}}$, which is in the range found by dye estimates; and $K_h > 1\,\mathrm{m^2\,s^{-1}}$ only for $r < 0.035$. With $\sigma_{\ln K} = 1.2$ and corr = 1 but no lognormality (thick dotted curve, Fig. 4), the horizontal diffusivity is smaller, with $K_h > 1\,\mathrm{m^2\,s^{-1}}$ only for intermittencies $r < 0.01$. For higher $\sigma_{\ln K} = 2.1$ and corr = 1 (Fig. 4), the predicted K_h rises above dye-inferred diffusivities for $r < 0.36$. For observed $r = 0.05$–0.1, K_h has diffusivities greater than or equal to dye estimates for $\sigma_{\ln K} > 1.8$. Horizontal diffusivities K_h exceed 1 for all intermittencies r if $\sigma_{\ln K}$ exceeds 2.4. Finally, assuming a lower-bound correlation corr = 0.6 (Peters et al. 1995) and $\sigma_{\ln K} = 1.2$ (thin solid curve, Fig. 4) produces horizontal diffusivities $K_h = 0.3$–$0.4\,\mathrm{m^2\,s^{-1}}$ for intermittencies $r = 0.05$–0.1 and $K_h > 1\,\mathrm{m^2\,s^{-1}}$ for intermittencies $r < 0.02$. We caution that, for $r \le 0.02$ (shading in Fig. 4), $\{K_z\}_b = \langle K_z\rangle/r$ is sufficiently high to violate the weak-mixing assumption used to justify the chosen z dependence in (7) because $\{K_z\}_b \delta t > m^{-2}$ for $\delta t \sim f^{-1}$, so that the turbulent events can wipe out the vertical structure on scales m^{-1}, short-circuiting horizontal mixing. The intermittency and lognormality introduced in (15) imply that the upper bound for

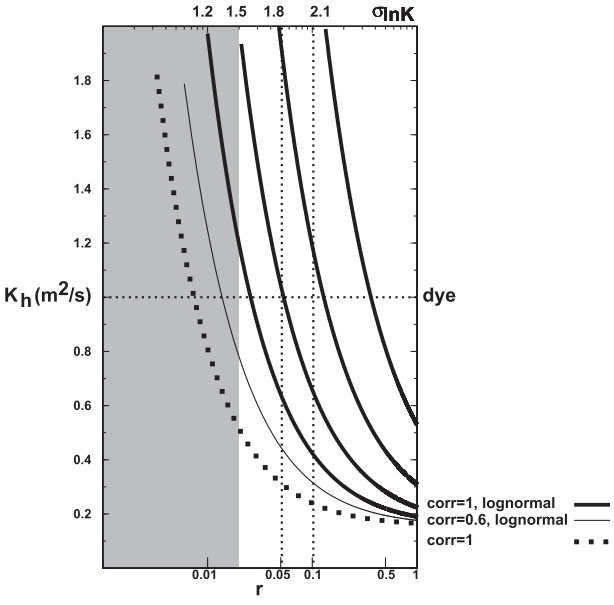

FIG. 4. Horizontal diffusivity K_h from (9) as a function of turbulent intermittency r assuming $\Delta z = 1$ m in (12), bulk average diapycnal diffusivity $K_0 = 0.05 \times 10^{-4}\,\mathrm{m^2\,s^{-1}}$, buoyancy frequency $N = 0.01\,\mathrm{rad\,s^{-1}}$, Coriolis frequency $f = 8 \times 10^{-5}\,\mathrm{rad\,s^{-1}}$, mixing efficiency $\gamma = 0.2$, and a critical gradient Froude number $\delta_c = 2$. Finescale parameterization [(12)] is used to relate shear V_z to diapycnal diffusivity K_z numerically. Thick solid curves correspond to K_z having a lognormal distribution [(14)] during the r fraction of time turbulence is present, with $\sigma_{\ln K}$ labeled along the upper axis and perfect correlation (corr = 1) between K_z and unstable shear variance $V_z^2 > \delta_c^2 N^2$. The thin solid curve uses a lower-bound correlation of 0.6 for $\sigma_{\ln K} = 1.2$ (Peters et al. 1995). The thick dotted curve assumes intermittency and perfect correlation but no lognormality, so it is independent of $\sigma_{\ln K}$. Horizontal diffusivity K_h increases as intermittency $r \to 0$, with lognormality and increasing $\sigma_{\ln K}$. Gray shading for $r < 0.02$ indicates where $\{K_z\}_b = \langle K_z\rangle/r$ is high enough to violate the weak-mixing approximation in (7) because $\{K_z\}_b \delta t > m^{-2}$ for durations $\delta t \sim f^{-1}$, but the impact of this remains to be assessed.

TABLE 1. Dependence of horizontal diffusivity K_h [(15)] on intermittency r and $\sigma_{\ln K}$ for corr = 1. The reported range of intermittency r is boldface in the second column. The reported dye diffusivities K_h are bold in the third column.

$\sigma_{\ln K}$	r ($K_h = 1\,\mathrm{m^2\,s^{-1}}$)	K_h ($r = 0.1$)	K_h ($r = 1$)
1.2	0.03	0.42	0.19
1.5	**0.05**	**0.66**	0.22
1.8	**0.13**	**1.19**	0.31
2.1	0.36	2.45	0.52

shear-dispersion-induced K_h derived by Young et al. (1982) no longer applies, particularly as $r \to 0$ or large $\sigma_{\ln K}$.

The conclusions above suggest that, within constraints of available observations, internal-wave shear dispersion cannot yet be ruled out as a possible explanation for the horizontal diffusivities K_h inferred from 1–5-km open-ocean dye studies. The key features for this argument are (i) the intermittency of ocean turbulence r, (ii) its probability density function [(14)], and (iii) its degree of correlation with finescale off-diagonal vertical strain $|\boldsymbol{\chi}_z| = |\int \mathbf{V}_z\,dt|$ (Fig. 4). The exact relationship [e.g., (12)] between K_z and V_z^2 is secondary, provided that K_z is an increasing function of V_z^2. While observations have established a clear relationship between turbulence and reduced shear (Peters et al. 1995; Polzin 1996; Jurisa et al. 2015, manuscript submitted to *J. Phys. Oceanogr.*), the relation between K_z and $|\boldsymbol{\chi}_z|^2$ is unknown and likely varies from one dynamic regime to another.

4. Summary

In the traditional application of internal-wave shear dispersion, either average turbulent diapycnal diffusivity $\langle K_z \rangle$, average variance of vertical shear $\langle V_z^2 \rangle$, or both have been used, essentially assuming that fluctuations in these two quantities are uncorrelated ($\langle K_z' V_z^{2\prime} \rangle = 0$ so that $\langle K_z V_z^2 \rangle = \langle K_z \rangle \langle V_z^2 \rangle$), resulting in a horizontal diffusivity $K_h \sim 0.1\,\mathrm{m^2\,s^{-1}}$. Here, we have explored the consequences of accounting for (i) the intermittency of ocean turbulence r, (ii) its lognormality [(14)], and (iii) its correlation with unstable finescale shear. An established parameterization [(12)] was used to relate vertical shear and turbulent mixing; any scaling where K_z increases with finescale V_z^2 would produce similar results, and this particular parameterization was chosen because it has strong observational support from finescale shear and microstructure measurements (Peters et al. 1995; Polzin 1996; Jurisa et al. 2015, manuscript submitted to *J. Phys. Oceanogr.*) Taken together and applied to the shear version of (15), a horizontal diffusivity $K_h \sim O(1)\,\mathrm{m^2\,s^{-1}}$ was found for $\sigma_{\ln K} = 1.2$ (Gregg et al. 1993), ocean intermittencies $r < 0.03$, and correlations corr > 0.6. These K_h are consistent with dye estimates in the stratified ocean interior (Ledwell et al. 1998; Sundermeyer and Ledwell 2001; D. A. Birch et al. 2015, unpublished manuscript). The conclusions are most sensitive to the intermittency r, probability density function for K_z [e.g., (14)], and the correlation between K_z and V_z^2 (Fig. 4; Table 1) with the exact model relating diapycnal diffusivity K_z and shear variance V_z^2 being secondary.

There are two major caveats. First, the PDF of K_z in the ocean is only approximately lognormal with deviations at high K_z which will impact K_h estimates from (15). While ocean sampling is sufficient to characterize the mean $\langle K_z \rangle$, standard deviations $\sigma_{\ln K}$ are rarely reported, let alone sufficient sampling for higher-order quantities like shear dispersion [(15)]. Second, while K_z and finescale shear variance V_z^2 appear to be well correlated, it is the correlation between K_z and the variance of off-diagonal vertical strain $|\boldsymbol{\chi}_z|^2$ that is relevant for shear dispersion, and this has not been characterized in the ocean. A third caveat is that the argument presented following (1) for the smallness of $K_z m^2/f$ in the ocean need not hold for intermittent mixing; horizontal dispersion can be short-circuited by elevated vertical mixing persisting for $\delta t \sim O(f^{-1})$ or longer as $r \to 0$ (shading in Fig. 4) as illustrated by (1).

Elevated horizontal diffusivities K_h due to shear dispersion hinge on unstable shear persisting for $O(f^{-1})$ so that the off-diagonal vertical strain $|\boldsymbol{\chi}_z| = |\int \mathbf{V}_z\,dt|$ can become large while diapycnal mixing K_z is strong [Fig. 5b; (11)]. Although the unstable-shear parameterization [(12)] implies rapid loss of unstable shears to turbulence on a time scale $4/(|\mathbf{V}_z| - \delta_c N) \sim O(N^{-1})$, which is too short for the creation of large vertical gradients of horizontal displacement $|\boldsymbol{\chi}_z|$ (Fig. 5a), microstructure observations often find that the strongest turbulent mixing can persist for days associated with near-inertial shear (Gregg et al. 1986; Sundermeyer et al. 2005). This implies that unstable shears must be continuously replenished by nonlinear wave–wave or wave–mean interactions (appendix) in order to maintain unstable shears $|\mathbf{V}_z|$ and turbulent diapycnal mixing K_z long enough to create large $|\boldsymbol{\chi}_z| \sim |\int \mathbf{V}_z\,dt|$ coincident with large K_z. Such persistent shear and mixing events should result in a strong correlation between K_z and $|\boldsymbol{\chi}_z| = |\int \mathbf{V}_z\,dt|$, which is an underlying assumption in our results, but this remains to be verified.

The statistics of both shear and turbulence may vary in different regions of the ocean. Thus, the effects discussed here will be of varying importance depending on the degree of correlation between K_z and finescale off-diagonal vertical strain $|\boldsymbol{\chi}_z| = |\int \mathbf{V}_z\,dt|$, so these must be

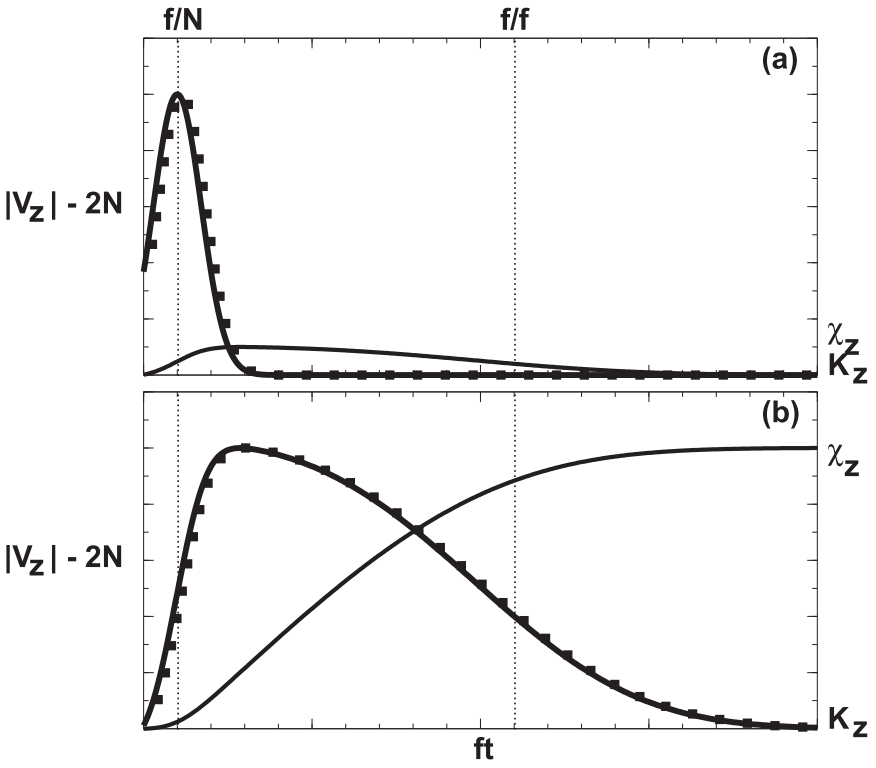

FIG. 5. Cartoon of two scenarios for shear dispersion, where the thick dotted curves represent unstable reduced shear $|\mathbf{V}_z| - 2N$, thick solid curves diapycnal diffusivity K_z, and thin solid curves the vertical gradient of horizontal displacement $|\boldsymbol{\chi}_z| = |\int \mathbf{V}_z\, dt|$. (a) The unstable shear and mixing decay over a buoyancy time scale $\delta t \sim N^{-1}$ so that $|\boldsymbol{\chi}_z|$ remains small. (b) Unstable shear and mixing persist over an inertial time scale $\delta t \sim f^{-1}$, allowing $|\boldsymbol{\chi}_z|$ to become large in conjunction with strong mixing.

resolved to correctly evaluate shear dispersion. In locales where turbulence and finescale shear are more uniform, such as seamount summits (Kunze and Toole 1997) and banks (Palmer et al. 2013), intermittency $r \sim 1$, so traditional shear dispersion $\langle K_z \rangle \langle V_z^2 \rangle / f^2$ will better reproduce true isopycnal mixing on the submesoscale. Likewise, traditional shear dispersion is expected to hold where K_z and $|\boldsymbol{\chi}_z|^2$ are uncorrelated or unstable shears do not persist long enough to produce significant $|\boldsymbol{\chi}_z| = |\int \mathbf{V}_z\, dt|$ coincident with elevated diapycnal mixing. However, where turbulence is intermittent ($r \ll 1$) and turbulence production is dominated by near-inertial wave packets, we anticipate that intermittency effects will be important to shear dispersion.

This paper has found that internal-wave shear dispersion is more subtle than previously recognized, depending not just on average diapynal diffusivities $\langle K_z \rangle$ and average shear variances $\langle V_z^2 \rangle$, but also on the time dependences and interdependences of these quantities. Our model horizontal diffusivities K_h are sensitive to the assumed lognormal probability distribution for K_z, which may not be a good description of ocean turbulence at the high K_z weighted by (15) (Gregg et al. 1993; Davis 1996). For these reasons, only observational assessment of the distribution of K_z and its correlation with the off-diagonal vertical strain $|\boldsymbol{\chi}_z| = |\int \mathbf{V}_z\, dt|$ will be able to address whether the proposed mechanism is important for shear dispersion in the ocean.

Acknowledgments. A. Sykulski, M. Inall, J. Ledwell, and an anonymous reviewer provided helpful comments. E. Kunze was supported by ONR Grant N00014-12-1-0942 and M. Sundermeyer by ONR Grant N00014-09-1-0194. In memoriam Murray Levine.

APPENDIX

Replenishment of Unstable Shear

Nonlinear wave–wave or wave–mean flow interactions can maintain unstable shear $V_z^2 > \delta_c^2 N^2$ by increasing the vertical wavenumber m or increasing the wave horizontal kinetic energy HKE,

$$\frac{\partial(V_z^2)}{\partial t} = 2\frac{\partial(m^2\mathrm{HKE})}{\partial t} = 4m\frac{\partial m}{\partial t}\mathrm{HKE} + 2m^2\frac{\partial \mathrm{HKE}}{\partial t}, \tag{A1}$$

where ray-tracing theory (Olbers 1981) suggests that

$$\frac{\partial m}{\partial t} = -kV_z = -m\sqrt{\omega^2 - f^2}\ \frac{V_z}{N} \tag{A2}$$

and

$$\frac{\partial(Cg_z\mathrm{HKE})}{\partial t} = \frac{\partial(Cg_z)}{\partial t}\mathrm{HKE} + Cg_z\frac{\partial(\mathrm{HKE})}{\partial t} = 0 \tag{A3}$$

for finescale near-inertial waves. This can be rewritten as

$$\frac{\partial(\mathrm{HKE})}{\partial t} = -\frac{1}{Cg_z}\frac{\partial(Cg_z)}{\partial t}\mathrm{HKE} = -\frac{1}{Cg_z}\frac{\partial(Cg_z)}{\partial m}\frac{\partial m}{\partial t}\mathrm{HKE}, \tag{A4}$$

where the vertical group velocity is

$$Cg_z = \frac{\partial\omega}{\partial m} = \frac{\partial(\sqrt{f^2 + N^2k^2/m^2})}{\partial m} = -\frac{N^2k^2}{m^3\sqrt{f^2 + N^2k^2/m^2}} \tag{A5}$$

and its derivative

$$\frac{\partial Cg_z}{\partial m} = \frac{N^2k^2}{m^3(f^2m^2 + N^2k^2)^{3/2}}(3f^2m^2 + 2N^2k^2) \tag{A6}$$

so that

$$\frac{1}{Cg_z}\frac{\partial Cg_z}{\partial m} = -\frac{(3f^2m^2 + 2N^2k^2)}{m(f^2m^2 + N^2k^2)} = \frac{2\omega^2 + f^2}{m\omega^2}. \tag{A7}$$

Combining (A1), (A2) and (A7)

$$\frac{\partial(V_z^2)}{\partial t} = \left(\frac{4\omega^2 + f^2}{\omega^2}\right)\sqrt{\omega^2 - f^2}\ \frac{V_z}{N}V_z^2 \sim cfV_z^2 \tag{A8}$$

with a growth rate of $O(f)$. We caution that the linear hydrostatic dispersion relation was used in conversion from horizontal wavenumber k and vertical group velocity Cg_z to vertical wavenumber m and frequency ω. This may not apply on the finescale; however, it should provide reasonable ballpark estimates. Comparing (A8) to the shear instability growth rate in (12) implies balance when

$$\frac{|V_z|}{N} \sim \frac{2N\omega^2}{N\omega^2 - 4(4\omega^2 + f^2)\sqrt{\omega^2 - f^2}} \tag{A9}$$

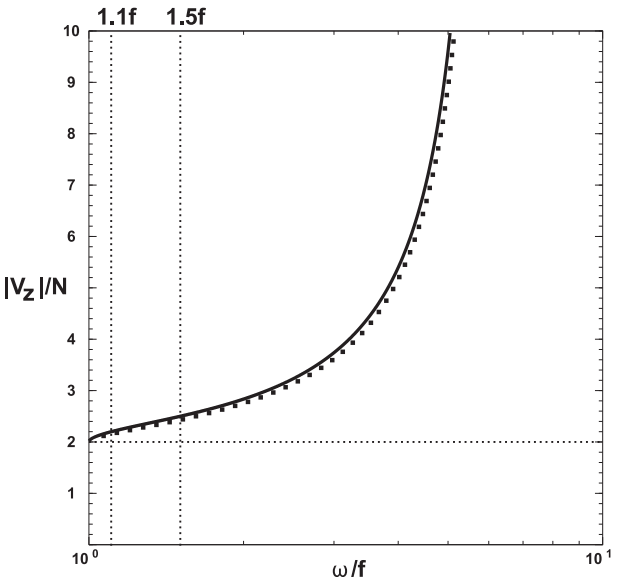

FIG. A1. Buoyancy-frequency-normalized shear $|V_z|/N$ vs Coriolis-frequency-normalized frequency ω/f to achieve a balance (solid curve) between shear variance amplification $(4\omega^2 + f^2)(\omega^2 - f^2)^{1/2}|\mathbf{V}_z|/(N\omega^2)$ [(A8)] and loss to turbulence $(|\mathbf{V}_z| - 2N)/4$ [(12)] as shown by (A9). The thick dotted curve shows the balance for only vertical shearing effects $(\omega^2 - f^2)^{1/2}|\mathbf{V}_z|/N$ vs $(|\mathbf{V}_z| - 2N)/4$ without wave dynamics [(A3)–(A7)], that is, omitting the second term on the right-hand side of (A1). The thin dotted horizontal line corresponds to the assumed critical $\delta_c = |\mathbf{V}_z|/N = 2$.

(Fig. A1). The curve is nearly identical if internal-wave dynamics is neglected, that is, only including the kinematics of dm/dt in the first term on the rhs of (A1) and neglecting the second term. This suggests the details of finescale wave dynamics are negligible compared to the kinematics of vertical shearing. For unstable near-inertial shears ($\omega < 2f$), a balance requires unstable shears $\delta_N = |\mathbf{V}_z|/N = 2$–3, consistent with finescale observations of unstable shear (Kunze et al. 1990b; Peters et al. 1995; Polzin 1996; Jurisa et al. 2015, manuscript submitted to *J. Phys. Oceanogr.*).

REFERENCES

Baker, M. A., and C. H. Gibson, 1987: Sampling turbulence in the stratified ocean: Statistical consequences of strong intermittency. *J. Phys. Oceanogr.*, **17**, 1817–1836, doi:10.1175/1520-0485(1987)017<1817:STITSO>2.0.CO;2.

Brunner-Suzuki, A.-M. E. G., M. A. Sundermeyer, and M.-P. Lelong, 2014: Upscale energy transfer induced by the vortical mode and internal waves. *J. Phys. Oceanogr.*, **44**, 2446–2469, doi:10.1175/JPO-D-12-0149.1.

Bühler, O., N. Grisouard, and M. Holmes-Certon, 2013: Strong particle dispersion by weakly dissipative random internal waves. *J. Fluid Mech.*, **719**, R4, doi:10.1017/jfm.2013.71.

Cole, S. T., and D. L. Rudnick, 2012: The spatial distribution and annual cycle of upper ocean thermohaline structure. *J. Geophys. Res.*, **117**, C02027, doi:10.1029/2011JC007033.

D'Asaro, E. A., and R.-C. Lien, 2000: The wave–turbulence transition for stratified flows. *J. Phys. Oceanogr.*, **30**, 1669–1678, doi:10.1175/1520-0485(2000)030<1669:TWTTFS>2.0.CO;2.

Davis, R. E., 1996: Sampling turbulent dissipation. *J. Phys. Oceanogr.*, **26**, 341–358, doi:10.1175/1520-0485(1996)026<0341:STD>2.0.CO;2.

Desaubies, Y., and W. K. Smith, 1982: Statistics of Richardson number and instability in oceanic internal waves. *J. Phys. Oceanogr.*, **12**, 1245–1259, doi:10.1175/1520-0485(1982)012<1245:SORNAI>2.0.CO;2.

Dillon, T. M., 1982: Vertical overturns: A comparison of Thorpe and Ozmidov scales. *J. Geophys. Res.*, **87**, 9601–9613, doi:10.1029/JC087iC12p09601.

Eriksen, C. C., 1978: Measurements and models of finestructure, internal gravity waves and wave breaking in the deep ocean. *J. Geophys. Res.*, **83**, 2989–3009, doi:10.1029/JC083iC06p02989.

Gargett, A. E., 1990: Do we really know how to scale the turbulent kinetic energy dissipation rate ε due to breaking of oceanic internal waves? *J. Geophys. Res.*, **95**, 15 971–15 974, doi:10.1029/JC095iC09p15971.

——, P. J. Hendricks, T. B. Sanford, T. R. Osborn, and A. J. Williams III, 1981: A composite spectrum of vertical shear in the upper ocean. *J. Phys. Oceanogr.*, **11**, 1258–1271, doi:10.1175/1520-0485(1981)011<1258:ACSOVS>2.0.CO;2.

Gregg, M. C., 1989: Scaling turbulent dissipation in the thermocline. *J. Geophys. Res.*, **94**, 9686–9698, doi:10.1029/JC094iC07p09686.

——, and T. B. Sanford, 1988: The dependence of turbulent dissipation on stratification in a diffusively stable thermocline. *J. Geophys. Res.*, **93**, 12 381–12 392, doi:10.1029/JC093iC10p12381.

——, E. A. D'Asaro, T. J. Shay, and N. Larson, 1986: Observations of persistent mixing and near-inertial internal waves. *J. Phys. Oceanogr.*, **16**, 856–885, doi:10.1175/1520-0485(1986)016<0856:OOPMAN>2.0.CO;2.

——, H. E. Seim, and D. B. Percival, 1993: Statistics of shear and turbulent dissipation profiles in random internal wave fields. *J. Phys. Oceanogr.*, **23**, 1777–1799, doi:10.1175/1520-0485(1993)023<1777:SOSATD>2.0.CO;2.

——, T. B. Sanford, and D. P. Winkel, 2003: Reduced mixing from the breaking of internal waves in equatorial waters. *Nature*, **422**, 513–515, doi:10.1038/nature01507.

Hazel, P., 1972: Numerical studies of the stability of inviscid stratified shear flows. *J. Fluid Mech.*, **51**, 39–61, doi:10.1017/S0022112072001065.

Henyey, F. S., J. Wright, and S. M. Flatté, 1986: Energy and action flow through the internal wave field: An eikonal approach. *J. Geophys. Res.*, **91**, 8487–8495, doi:10.1029/JC091iC07p08487.

Inall, M. E., D. Aleynik, and C. Neil, 2013: Horizontal advection and dispersion in a stratified sea: The role of inertial oscillations. *Prog. Oceanogr.*, **117**, 25–36, doi:10.1016/j.pocean.2013.06.008.

Itsweire, E. C., T. R. Osborn, and T. P. Stanton, 1989: Horizontal distribution and characteristics of shear layers in the seasonal thermocline. *J. Phys. Oceanogr.*, **19**, 301–320, doi:10.1175/1520-0485(1989)019<0301:HDACOS>2.0.CO;2.

——, J. R. Koseff, D. A. Briggs, and J. H. Ferziger, 1993: Turbulence in stratified shear flows: Implications for interpreting shear-induced mixing in the ocean. *J. Phys. Oceanogr.*, **23**, 1508–1522, doi:10.1175/1520-0485(1993)023<1508:TISSFI>2.0.CO;2.

Kundu, P. K., and I. M. Cohen, 2004: *Fluid Mechanics*. Elsevier, 759 pp.

Kunze, E., 1993: Submesocale dynamics near a seamount. Part II: The partition of energy between internal waves and geostrophy. *J. Phys. Oceanogr.*, **23**, 2589–2601, doi:10.1175/1520-0485(1993)023<2589:SDNASP>2.0.CO;2.

——, 2014: The relation between unstable shear layer thicknesses and turbulence lengthscales. *J. Mar. Res.*, **72**, 95–104, doi:10.1357/002224014813758977.

——, and T. B. Sanford, 1993: Submesoscale dynamics near a seamount. Part I: Measurements of Ertel vorticity. *J. Phys. Oceanogr.*, **23**, 2567–2588, doi:10.1175/1520-0485(1993)023<2567:SDNASP>2.0.CO;2.

——, and J. M. Toole, 1997: Tidally driven vorticity, diurnal shear, and turbulence atop Fieberling Seamount. *J. Phys. Oceanogr.*, **27**, 2663–2693, doi:10.1175/1520-0485(1997)027<2663:TDVDSA>2.0.CO;2.

——, M. G. Briscoe, and A. J. Williams III, 1990a: Interpreting shear and strain finestructure from a neutrally buoyant float. *J. Geophys. Res.*, **95**, 18 111–18 125, doi:10.1029/JC095iC10p18111.

——, A. J. Williams III, and M. G. Briscoe, 1990b: Observations of shear and vertical stability from a neutrally buoyant float. *J. Geophys. Res.*, **95**, 18 127–18 142, doi:10.1029/JC095iC10p18127.

——, J. M. Klymak, R.-C. Lien, R. Ferrari, C. M. Lee, M. A. Sundermeyer, and L. Goodman, 2015: Submesoscale water-mass spectra in the Sargasso Sea. *J. Phys. Oceanogr.*, **45**, 1325–1338, doi:10.1175/JPO-D-14-0108.1.

Ledwell, J. R., A. J. Watson, and C. S. Law, 1998: Mixing of a tracer in the pycnocline. *J. Geophys. Res.*, **103**, 21 499–21 529, doi:10.1029/98JC01738.

Lelong, M.-P., and M. A. Sundermeyer, 2005: Geostrophic adjustment of an isolated diapycnal mixing event and its implications for small-scale lateral dispersion. *J. Phys. Oceanogr.*, **35**, 2352–2367, doi:10.1175/JPO2835.1.

——, ——, and E. Kunze, 2002: Numerical simulations of lateral dispersion by the relaxation of diapycnal mixing events. *Eos, Trans. Amer. Geophys. Union*, **83** (Meeting Suppl.), Abstract OS31O-08.

Lumpkin, R., and S. Elipot, 2010: Surface drifter pair spreading in the North Atlantic. *J. Geophys. Res.*, **115**, C12017, doi:10.1029/2010JC006338.

MacKinnon, J. A., and M. C. Gregg, 2003: Mixing on the late-summer New England shelf—Solibores, shear, and stratification. *J. Phys. Oceanogr.*, **33**, 1476–1492, doi:10.1175/1520-0485(2003)033<1476:MOTLNE>2.0.CO;2.

Marmorino, G. O., J. P. Dugan, and T. E. Evans, 1986: Horizontal variability of microstructure in the vicinity of a Sargasso Sea front. *J. Phys. Oceanogr.*, **16**, 967–986, doi:10.1175/1520-0485(1986)016<0967:HVOMIT>2.0.CO;2.

——, L. J. Rosenblum, and C. L. Trump, 1987: Finescale temperature variability: The influence of near-inertial waves. *J. Geophys. Res.*, **92**, 13 049–13 069, doi:10.1029/JC092iC12p13049.

Mellor, G. L., and T. Yamada, 1982: Development of a turbulence closure model for geophysical fluid problems. *Rev. Geophys.*, **20**, 851–875, doi:10.1029/RG020i004p00851.

Molemaker, M. J., J. C. McWilliams, and X. Capet, 2010: Balanced and unbalanced routes to dissipation in an equilibrated Eady flow. *J. Fluid Mech.*, **654**, 35–63, doi:10.1017/S0022112009993272.

Moniz, R. J., D. A. Fong, C. B. Woodson, S. K. Willis, M. T. Stacey, and S. G. Monismith, 2014: Scale-dependent dispersion within the stratified interior on the shelf of northern Monterey Bay. *J. Phys. Oceanogr.*, **44**, 1049–1064, doi:10.1175/JPO-D-12-0229.1.

Moum, J. N., 1996: Energy-containing scales of turbulence in the ocean thermocline. *J. Geophys. Res.*, **101**, 14 095–14 109, doi:10.1029/96JC00507.

Müller, P., 1984: Small-scale vortical motions. *Internal Gravity Waves and Small Scale Turbulence: Proc. 'Aha Huliko'a*

Hawaiian Winter Workshop, Honolulu, HI, University of Hawai'i at Mānoa, 249–262.

——, R.-C. Lien, and R. Williams, 1988: Estimates of potential vorticity at small scales in the ocean. *J. Phys. Oceanogr.*, **18**, 401–416, doi:10.1175/1520-0485(1988)018<0401:EOPVAS>2.0.CO;2.

Olbers, D. J., 1981: The propagation of internal waves in a geostrophic current. *J. Phys. Oceanogr.*, **11**, 1224–1233, doi:10.1175/1520-0485(1981)011<1224:TPOIWI>2.0.CO;2.

Osborn, T. R., 1980: Estimates of the local rate of diffusion form dissipation measurements. *J. Phys. Oceanogr.*, **10**, 83–89, doi:10.1175/1520-0485(1980)010<0083:EOTLRO>2.0.CO;2.

Palmer, M. R., M. E. Inall, and J. Sharples, 2013: The physical oceanography of Jones Bank: A mixing hotspot in the Celtic Sea. *Prog. Oceanogr.*, **117**, 9–24, doi:10.1016/j.pocean.2013.06.009.

Peters, H., M. C. Gregg, and T. B. Sanford, 1995: On the parameterization of equatorial turbulence: Effect of finescale variations below the range of the diurnal cycle. *J. Geophys. Res.*, **100**, 18 333–18 348, doi:10.1029/95JC01513.

Pinkel, R., 2014: Vortical and internal wave shear and strain. *J. Phys. Oceanogr.*, **44**, 2070–2092, doi:10.1175/JPO-D-13-090.1.

Poje, A. C., and Coauthors, 2014: Submesoscale dispersion in the vicinity of the *Deepwater Horizon* spill. *Proc. Natl. Acad. Sci. USA*, **111**, 12 693–12 698, doi:10.1073/pnas.1402452111.

Polzin, K. L., 1996: Statistics of the Richardson number: Mixing models and finestructure. *J. Phys. Oceanogr.*, **26**, 1409–1425, doi:10.1175/1520-0485(1996)026<1409:SOTRNM>2.0.CO;2.

——, J. M. Toole, and R. W. Schmitt, 1995: Finescale parameterization of turbulent dissipation. *J. Phys. Oceanogr.*, **25**, 306–328, doi:10.1175/1520-0485(1995)025<0306:FPOTD>2.0.CO;2.

——, E. Kunze, J. M. Toole, and R. W. Schmitt, 2003: The partition of finescale energy into internal waves and subinertial motions. *J. Phys. Oceanogr.*, **33**, 234–248, doi:10.1175/1520-0485(2003)033<0234:TPOFEI>2.0.CO;2.

Rohr, J. J., E. C. Itsweire, K. N. Helland, and C. W. Van Atta, 1988: Growth and decay of turbulence in a stably stratified shear flow. *J. Fluid Mech.*, **195**, 77–111, doi:10.1017/S0022112088002332.

Rudnick, D., and R. Ferrari, 1999: Compensation of horizontal temperature and salinity gradients in the ocean mixed layer. *Science*, **283**, 526–529, doi:10.1126/science.283.5401.526.

Scotti, R. S., and G. M. Corcos, 1972: An experiment on the stability of small disturbances in a stratified free-shear layer. *J. Fluid Mech.*, **52**, 499–528, doi:10.1017/S0022112072001569.

Shcherbina, A. Y., and Coauthors, 2015: The LatMix summer campaign: Submesoscale stirring in the upper ocean. *Bull. Amer. Meteor. Soc.*, **96**, 1257–1279, doi:10.1175/BAMS-D-14-00015.1.

Smith, S., and R. Ferrari, 2009: The production and dissipation of compensated thermohaline variance by mesoscale stiriring. *J. Phys. Oceanogr.*, **39**, 2477–2501, doi:10.1175/2009JPO4103.1.

Sun, H., and E. Kunze, 1999: Internal wave–wave interactions. Part I: The role of internal wave vertical divergence. *J. Phys. Oceanogr.*, **29**, 2886–2904, doi:10.1175/1520-0485(1999)029<2886:IWWIPI>2.0.CO;2.

Sundermeyer, M. A., and J. R. Ledwell, 2001: Lateral dispersion over the continental shelf: Analysis of dye-release experiments. *J. Geophys. Res.*, **106**, 9603–9621, doi:10.1029/2000JC900138.

——, and M.-P. Lelong, 2005: Numerical simulations of lateral dispersion by the relaxation of diapycnal mixing events. *J. Phys. Oceanogr.*, **35**, 2368–2386, doi:10.1175/JPO2834.1.

——, J. R. Ledwell, N. S. Oakey, and B. J. W. Greenan, 2005: Stirring by small-scale vortices caused by patchy mixing. *J. Phys. Oceanogr.*, **35**, 1245–1262, doi:10.1175/JPO2713.1.

Thorpe, S. A., 1971: Experiments on the instability of stratified shear flows: Miscible flows. *J. Fluid Mech.*, **46**, 299–319, doi:10.1017/S0022112071000557.

Toole, J. M., and R. W. Schmitt, 1987: Small-scale structures in the north-west Atlantic sub-tropical front. *Nature*, **327**, 47–49, doi:10.1038/327047a0.

Young, W. R., P. B. Rhines, and C. J. R. Garrett, 1982: Shear-flow dispersion, internal waves and horizontal mixing in the ocean. *J. Phys. Oceanogr.*, **12**, 515–527, doi:10.1175/1520-0485(1982)012<0515:SFDIWA>2.0.CO;2.